

A Vibrational Analysis on Possible Peroxo Forms of Soluble Methane Monooxygenase

Takashi Yumura[1,2] **and Kazunari Yoshizawa***[,1]

[1]Institute for Materials Chemistry and Engineering, Kyushu University, Fukuoka 812-8581

[2]Department of Materials Science and Engineering, Meijo University, Tenpaku-ku, Nagoya 468-8502

Received January 14, 2004; E-mail: kazunari@ms.ifoc.kyushu-u.ac.jp

The vibrational structures for two possible peroxo intermediates of soluble methane monooxygenase (sMMO), in which O_2 binds into the diiron(II) active site with end-on and side-on bridging modes, are analyzed from quantum chemical calculations at the B3LYP DFT level of theory. Dioxygen bridging modes should be controlled by carboxylate coordinations around the diiron active site. Two bridging carboxylato ligands are contained in the end-on peroxo complex, whereas one bridging carboxylato ligand is contained in the side-on peroxo complex. DFT calculations demonstrate that the end-on bridging mode into the diiron active site is energetically more stable than the side-on bridging mode. The end-on peroxo complex has a vibrational mode of O–O stretching at 909 cm^{-1}, the isomer shift of which upon $^{18}O_2$ substitution is 57 cm^{-1}. The side-on peroxo complex exhibits a lower O–O stretching mode at 841 cm^{-1}, and the isotope shift is 45 cm^{-1}. The frequency of the O–O stretching mode and the $^{18}O_2$ isotope shift are dependent on the dioxygen bridging modes in the active site of sMMO. The O–O stretching frequency in the end-on complex falls within the range measured in peroxo intermediates of other non-heme diiron enzymes and *cis*-μ-1,2 peroxo-bridged diiron(III) synthetic complexes. From the viewpoint of energetics and the vibrational frequencies, it is predicted that O_2 should coordinate into the diiron active site of sMMO in an end-on *cis*-μ-1,2 fashion rather than a side-on fashion.

Methane monooxygenase (MMO) catalyzes the transformation of CH_4 and O_2 into CH_3OH and H_2O at ambient pressure and temperature.[1] As the active site for dioxygen activation and methane hydroxylation, a carboxylate-bridged diiron center is located in the α subunit of the hydroxylase protein (MMOH). In the first stages of the catalytic function, O_2 is incorporated into the reduced MMOH ($MMOH_{red}$) with the oxidation state of Fe(II)Fe(II).[2] Since $MMOH_{red}$ has five-coordinate iron atoms as a result of a carboxylate shift of Glu243,[2d–f] such a coordinatively unsaturated diiron center affords a binding site for O_2. The versatility of carboxylate coordination brings greater flexibility to the diiron active site, making it possible to bind O_2 in a bridging fashion. After that the O–O bond is activated, resulting in the formation of the peroxo Fe(III)Fe(III) intermediate $MMOH_{peroxo}$ that has been characterized by stopped-flow optical absorption (broad band centered at $\sim$700 nm, $\varepsilon_{700} \approx 1500$ M^{-1} cm^{-1}) and rapid freeze-quench Mössbauer spectroscopies ($\delta = 0.66$ mm/s, $\Delta E_Q = 1.5$ mm/s for both irons).[3] The $MMOH_{peroxo}$ intermediate, in which the two iron atoms are antiferromagnetically coupled, subsequently converts to the high-valent Fe(IV)Fe(IV) intermediate $MMOH_Q$ that has a direct reactivity toward substrate methane. The mechanisms for dioxygen activation and methane hydroxylation are under debate at present.

With regard to the mechanism of dioxygen activation on MMOH, structural features of $MMOH_{peroxo}$ are still lacking. Although resonance Raman spectroscopy gives important information on the unknown dioxygen binding mode in the diiron active site, no reliable data have yet been obtained for $MMOH_{peroxo}$. On the other hand, high O–O frequencies in the range of 850 and 900 cm^{-1} were detected in the diiron peroxo intermediates of stearoyl-acyl carrier protein Δ^9-desaturase,[4] frog ferritin,[5] and a mutant form of the R_2 subunit of ribonucleotide reductase (RNR-R2-D84E).[6] Because of spectroscopic similarities, the peroxo species in RNR-R2-D84E ($\delta = 0.63$ mm/s, $\Delta E_Q = 1.58$ mm/s for both irons in association with a broad optical absorption band at $\sim$700 nm) is considered to be strikingly similar to that in MMOH.[7]

Synthetic complexes play an important role in creating structural, spectroscopic, and mechanistic insights into the roles of the active sites in the non-heme diiron enzymes.[8–12] Suzuki et al.,[8] Que et al.,[9] and Lippard et al.[10] have characterized crystallographically *cis*-μ-1,2 peroxo-bridged diiron(III) complexes as synthetic models of $MMOH_{peroxo}$. The three complexes exhibit optical spectra similar to that of $MMOH_{peroxo}$. Resonance Raman studies on the peroxo diiron(III) complexes suggest that the Fe–O stretching modes fall in the range of 415–480 cm^{-1}, and the O–O stretching mode 850–900 cm^{-1}.[8–12] Solomon et al. investigated vibrational frequencies for a *cis*-μ-1,2 peroxo-bridged diiron(III) complex from a normal coordinate analysis (NCA) calculation.[12b] The analysis is based on the Wilson's FG-matrix method using a Urey–Bradley force field. According to the NCA calculation, the high O–O stretching frequency (876 cm^{-1}) in the *cis*-μ-1,2 peroxo-bridged diiron(III) complex results from substantial mechanical coupling between the Fe–O and O–O stretching motions.[12] These data are in good agreement with those in the non-heme peroxo diiron intermediates,[4–6] which indicates that O_2 binds into the dinuclear iron(II) active site in an end-on μ-1,2 fashion rather than a side-on fashion in the non-heme diiron enzymes.

Published on the web July 9, 2004; DOI 10.1246/bcsj.77.1305

Recent quantum chemical calculations have given useful information on the veiled catalytic cycle of MMOH, especially methane hydroxylation by $MMOH_Q$.[13–16] Siegbahn[14c] and Friesner et al.[16a] obtained from B3LYP density functional theory (DFT) calculations peroxo diiron complexes with a side-on bridging mode as $MMOH_{peroxo}$. Morokuma et al. have proposed that O_2 can bind in an end-on and a side-on manners into *cis*-$[(H_2O)(NH_2)Fe(\eta^2\text{-}HCOO)_2Fe(NH_2)(H_2O)]$.[15f] Despite experimental and theoretical researches, it is not yet clear in what fashion O_2 binds into the diiron active site of MMOH. In this study we report detailed vibrational analyses of two peroxo diiron(III) complexes as models of $MMOH_{peroxo}$ from the viewpoint of quantum chemical calculations to increase our understanding of the unknown structural and spectroscopic features of $MMOH_{peroxo}$.

Method of Calculation

In order to reproduce the observed antiferromagnetic state of the diiron complex of $MMOH_{peroxo}$,[3] we carried out quantum chemical calculations with a combination of the B3LYP method[17,18] and the broken-symmetry approach[19] available in the Gaussian 98 ab initio program package.[20] The broken-symmetry methodology[19] is based on unrestricted Hartree–Fock or DFT calculations for spin-singlet open shell systems in which spin-up and spin-down electrons are allowed to localize on different atomic centers. The broken-symmetry state is not a pure spin state described by a single determinant, but rather a weighted average of pure spin states to give a spin-coupling pattern with such an antiferromagnetic alignment. The energy of a broken-symmetry state is usually above but close to the true ground-state energy.[19] This methodology has been successfully used to describe a large number of magnetically coupled centers in metalloproteins.[21,22]

If the active site of $MMOH_{peroxo}$ involves a kind of edge-shared six-coordinate diiron(III) complex, this electronic feature is basically described in Chart 1. When an iron atom is coordinatively saturated, the relevant d-orbitals are divided into three low-lying t_{2g} orbitals and two high-lying e_g orbitals. Thus, the low-lying and high-lying blocks at the diiron active center are composed of six "t_{2g}" and four "e_g" orbitals, respectively. In the presence of excess spin-up or spin-down electron densities, spin-polarization results in a splitting of the d-blocks, as shown in Chart 1. In the weak iron–iron interaction limit, each iron-based electron remains substantially localized on one iron atom or the other. The broken-symmetry approach always describes electronic states in the weakly-coupled limit, and the spin singlet ground state arises through the antiparallel coupling of the spins on opposite centers.

The B3LYP method consists of the Slater exchange, the Hartree–Fock exchange, the exchange functional of Becke,[17] the correlation functional of Lee, Yang, and Parr (LYP),[18] and the correlation functional of Vosko, Wilk, and Nusair (VWN).[23] We used the triple–ζ–valence (TZV) basis set[24] for the two iron atoms, the TZV basis set with polarization functions (TZVP) for the peroxo ligand, and the 3-21G basis set[25–27] for the other H, C, N, and O atoms that are involved in the amino acid residues around the diiron active site (BS-I). Next, we replaced the TZVP basis set for the peroxo ligand with the TZV basis set to look at the significance of the polarization functions on the geometries and energetics of $MMOH_{peroxo}$ (BS-II). We modeled the glutamate and histidine residues around the diiron active site by formate and imidazole ligands, respectively. As a consequence, four formato, two imidazole, and one aqua ligands are involved in the diiron active site models of $MMOH_{peroxo}$. The geometries of the diiron model complexes were fully optimized, and the harmonic vibrational frequencies were calculated by the analytical evaluation of the second derivatives of the energy with respect to nuclear displacement. The models of $MMOH_{peroxo}$ contain 41 atoms, and hence they have 117 vibrational degrees of freedom. The Hartree–Fock (HF) method is known to systematically overestimate fundamental frequencies by 10–15% because of the neglect of electron correlation.[28a] In contrast, the B3LYP method reasonably estimates fundamental frequencies within accuracy of 2–3%, and hence B3LYP harmonic frequencies provide more reliable theoretical vibrational spectra in general.[28] Single-point energy calculations were also carried out at the B3LYP/TZV level of theory.

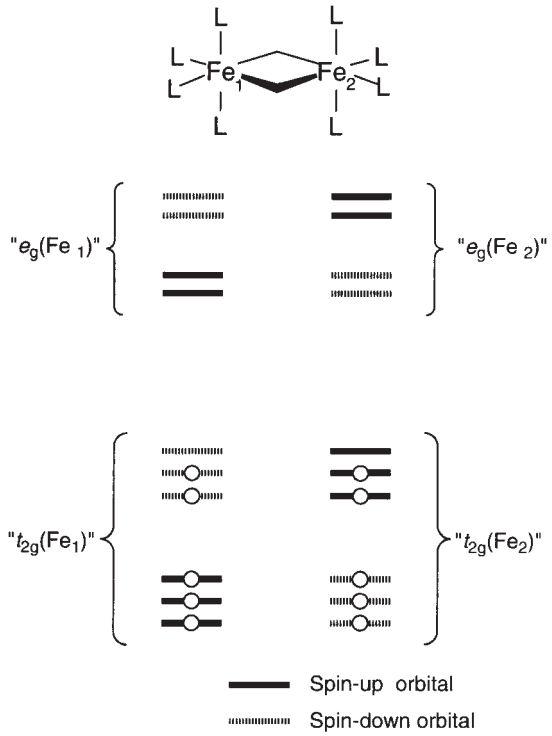

Chart 1.

Results and Discussion

The geometries of two possible dioxygen intermediates as models of $MMOH_{peroxo}$ were obtained at the B3LYP/BS-I level of theory; one is an end-on peroxo complex **1**[29] with a *cis*-μ-1,2 bridging mode and the other is a side-on peroxo complex **2**,[30] as shown in Fig. 1. The coordinate environments in the dioxygen intermediates correspond to that observed from X-ray crystallographic analyses. However, we tried in vain to optimize an end-on peroxo form with a *trans*-μ-1,2 bridging mode, although this form was actually detected in a synthetic diiron complex without bridging ligands.[31] Since the bridging carboxylato ligand holds the two iron centers short, O_2 cannot bind into the diiron active center in a *trans*-μ-1,2 fashion.

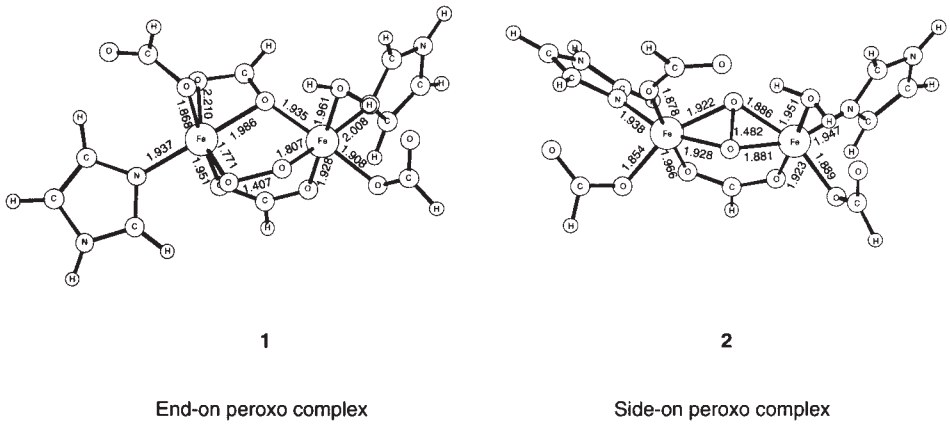

Fig. 1. Optimized geometries of end- and side-on peroxo diiron(III) complexes as models of the active site of $MMOH_{peroxo}$ from DFT B3LYP calculations. Bond lengths are in Å.

Table 1. Relative Energies of the Dioxygen Intermediates are Given in kcal/mol

	B3LYP/BS-I	B3LYP/BS-II
End-on peroxo complex **1**	0.0	0.0
Side-on peroxo complex **2**	13.0	12.6
End-on peroxo complex **3**	6.0	5.9
Side-on peroxo complex **4**	8.3	8.3

In the basis set system (BS-I), the triple–ζ–valence (TZV) basis set[24] is used for the two iron atoms, the TZV plus polarization (TZVP) basis set for the peroxo ligand, and the 3-21G basis set[25–27] for the other H, C, N, and O atoms that are involved in the amino acid residues around the diiron active site. In the basis set system (BS-II), the TZVP basis set for the peroxo ligand is replaced by the TZV basis set in BS-I.

The end-on peroxo complex **1** with the *cis*-μ-1,2 bridging mode has a doubly bridged structure with two carboxylato ligands. In this complex the O–O length is 1.407 Å, and the Fe–O lengths are 1.771 and 1.807 Å. A similar dioxygen bridging mode into *cis*-$(H_2O)(NH_2)Fe(\eta^2\text{-}HCOO)_2Fe(NH_2)(H_2O)$ was suggested by Morokuma et al.[15f] As seen in Fig. 1, **1** has a carboxylato ligand that serves as a bidentate, chelating ligand to the left-side iron atom; at the same time it is a monodentate bridging ligand between the two iron atoms. In contrast to **1**, the side-on peroxo complex **2** with a butterfly structure does not have such a carboxylato ligand. Because of the carboxylato ligand, the Fe–Fe separation in **2** (3.323 Å) is larger than that in **1** (3.148 Å). The difference in the Fe–Fe separations should result in lengthening O–O length (1.482 Å) and Fe–O lengths (~1.9 Å) in **2** relative to **1**. Thus, the carboxylato ligand coordination should be responsible for controlling the dioxygen bridging modes in $MMOH_{peroxo}$. As shown in Table 1, **2** is 13.0 kcal/mol more unstable than **1**. Single-point energy calculations at the B3LYP/TZV level of theory indicate a tendency in line with those at the B3LYP/BS-I level of theory; **1** lies 5.0 kcal/mol below **2**. Siegbahn proposed a side-on peroxo complex similar to ours,[14b,c] and Morokuma also obtained a peroxo diiron complex with a similar bridging mode.[15f] Friesner et al. proposed that O_2 binds in an asymmetric side-on fashion in $MMOH_{peroxo}$.[16a] To the best of our knowledge, peroxo diiron complexes with a μ-η^2:η^2 bridging mode have not yet been observed, whereas it was reported that O_2 binds in a side-on bridging mode into the dicopper active sites of oxytyrosinase,[31] oxyhemocyanin,[32,33] and synthetic dicopper complexes.[34–37]

We also obtained peroxo complexes **3** and **4** at the B3LYP/BS-I level of theory, as shown in Fig. 2. In **3** and **4**, the imidazole ligand and a formate ligand are replaced at the left-hand iron atom in the peroxo complexes **1** and **2**, respectively. Lippard et al. have suggested that the coordination environment at the left-side iron atom is much more flexible than that at the right-side iron atom.[2f] Accordingly, when the protein environment is taken into account, the dioxygen intermediates **3** and **4** can be regarded as possible isomers of the peroxo models in MMOH, although there remain of course many possibilities of diiron peroxo complexes. The O–O bond length in **3** with the *cis*-μ-1,2 bridging mode was calculated to be 1.413 Å, and that in **4** with the μ-η^2:η^2 bridging mode to be 1.480 Å. **3** and **4** have a Fe_2O_2 core similar to **1** and **2**, respectively, suggesting that the effect of the ligand exchanges is not significant. The present DFT calculations show that the end-on peroxo complex **1** is the most stable in energy in the dioxygen intermediates, as summarized in Table 1.

In the next section, we confine our discussions to the peroxo complexes **1** and **2** as models for $MMOH_{peroxo}$. Calculated spin densities on the iron atoms in **1** and **2** are approximately +1.0 and −1.0 in the broken-symmetry singlet state, as presented in Chart 2. On the other hand, the oxygen atoms in **1** and **2** do not have spin densities, suggesting that the electronic configuration of O_2^{2-} $(\sigma_u)^2(\pi_u)^4(\pi_g^*)^4(\sigma_g^*)^0$ should be involved in **1** and **2**. Since the iron atoms in the diiron(III) peroxo complexes are octahedrally coordinated, the relevant d-orbitals split into six "t_{2g}" and four "e_g" orbitals, as shown in Chart 1. If the sepa-

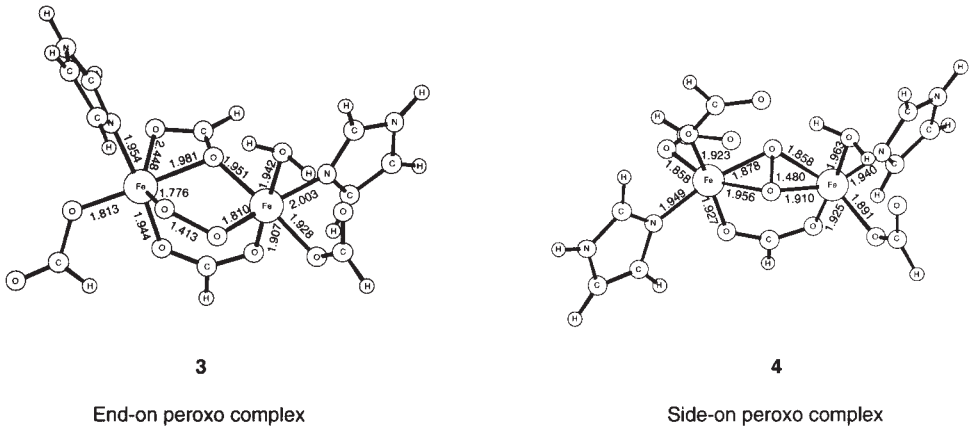

Fig. 2. Optimized geometries of isomers of the peroxo complexes from DFT B3LYP calculations. Bond lengths are in Å.

Chart 2.

Chart 3.

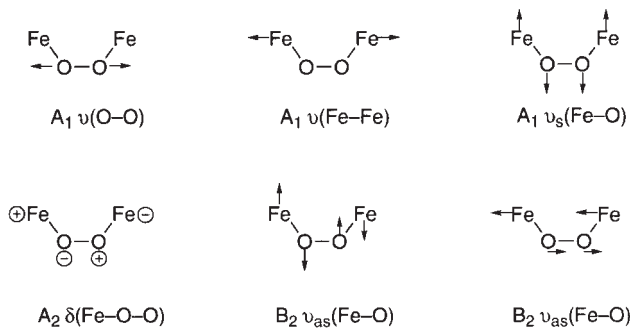

Fig. 3. Vibrational modes of the Fe_2O_2 core in an end-on peroxo complex are estimated from a simple symmetric consideration. ν represents stretches of bonds and δ represents bending.

ration between the "e_g" and "t_{2g}" blocks is large enough, the low-lying "t_{2g}" block should be occupied by ten d-electrons in the diiron(III) peroxo complexes. Three spin-up and two spin-down electrons are housed at one iron center, and two spin-up and three spin-down electrons are housed at the other iron center. Thus, the calculated spin distributions are reasonable. This result is different from those obtained by Friesner et al.; the antiferromagnetic state between the high-spin iron atoms was obtained from the Jaguar program.[16g]

Let us next pay attention to calculated vibrational frequencies for the peroxo complexes **1** and **2**. The Fe_2O_2 units for both peroxo complexes have nearly C_{2v} geometries, which are schematically represented in Chart 3. We can estimate vibrational modes in the end-on and side-on peroxo complexes from symmetry analyses[38] of the Fe_2O_2 units with ideal C_{2v} geometries. This symmetry consideration of the Fe_2O_2 cores should give us helpful hints for the understanding of the vibrational structures obtained from the DFT calculations.[31a,39]

Assuming that the Fe_2O_2 core with the end-on *cis*-μ-1,2 bridging mode has a C_{2v} geometry, the core has six vibrational degrees of freedom: three A_1, one A_2, and two B_1 normal modes that are Raman active, as shown in Fig. 3. The three A_1 modes are classified into O–O and Fe–Fe stretching and a symmetric combination of Fe–O stretching. The A_2 and B_1 modes involve out-of-plane bending and an antisymmetric combination of Fe–O stretching, respectively.

Oxygen-isotope sensitive vibrations for the end-on and side-on peroxo complexes obtained at the B3LYP/BS-I and B3LYP/BS-II levels of theory are shown in Tables 2 and 3, respectively. Tables 2 and 3 show significant dependence of the vibrational frequencies on the polarization functions for the peroxo ligands, although the energy separations are not significantly dependent on the polarization functions. As shown in Table 2, the end-on peroxo complex **1** has three oxygen-isotope sensitive vibrations; symmetric and antisymmetric combinations of the Fe–O stretching modes, and an O–O stretching mode. A vibrational mode at 909 cm^{-1}, which is shifted to 876 and 852 cm^{-1} with $^{16}O^{18}O$ and $^{18}O_2$ substitutions, respectively, is assigned to an O–O stretching mode in **1**. This corresponds to the left-side A_1 mode in Fig. 3. This value falls within the O–O stretching frequency range reported for the peroxo intermediates in non-heme diiron enzymes[4–6] and *cis*-μ-1,2 peroxo-bridged diiron(III) model complexes (850–900 cm^{-1}),[8–12] and hence this result justifies the vibrational analysis at this level of theory. The frequencies of the symmetric and antisymmetric combinations of the Fe–O stretching modes were computed to be 596 and 683 cm^{-1}, respectively. The $^{18}O_2$ isotope shift for the vibrational mode at 596 cm^{-1} is 17 cm^{-1}, and that for the mode at 683 cm^{-1} is 30 cm^{-1}.

The Fe_2O_2 core with the side-on bridging mode has six vibrational degrees of freedom, as shown in Fig. 4: three A_1, one A_2, one B_1, and one B_2 modes. All vibrational modes are Raman active. The three A_1 normal modes correspond to O–O and Fe–Fe stretching and butterfly modes. The A_2 and B_2 modes are assigned to symmetric and antisymmetric combina-

Table 2. Computed Frequencies (cm^{-1}) for Oxygen-Isotope Sensitive Modes in the End-on Peroxo Diiron(III) Model **1** of $MMOH_{peroxo}$

Modes	B3LYP/BS-I			B3LYP/BS-II		
	$^{16}O_2$	$^{16}O^{18}O$	$^{18}O_2$	$^{16}O_2$	$^{16}O^{18}O$	$^{18}O_2$
ν(O–O)	909	876	852	871	852	824
ν_{as}(Fe–O)	683	663	653	660	641	631
ν_s(Fe–O)	596	590	579	585	578	569

In the basis set system (BS-I), the triple–ζ–valence (TZV) basis set[24] is used for the two iron atoms, the TZV plus polarization (TZVP) basis set for the peroxo ligand, and the 3-21G basis set[25–27] for the other H, C, N, and O atoms that are involved in the amino acid residues around the diiron active site. In the basis set system (BS-II), the TZVP basis set for the peroxo ligand is replaced by the TZV basis set in BS-I.

Table 3. Computed Frequencies (cm^{-1}) for Oxygen-Isotope Sensitive Modes in the Side-on Peroxo Diiron(III) Model **2** of $MMOH_{peroxo}$

Modes	B3LYP/BS-I			B3LYP/BS-II		
	$^{16}O_2$	$^{16}O^{18}O$	$^{18}O_2$	$^{16}O_2$	$^{16}O^{18}O$	$^{18}O_2$
ν(O–O)	841	818	796	800	781	751
ν_{as}(Fe–O)	639	626	614	637	625	612
ν_s(Fe–O)	506	498	493	495	483	475
δ(Fe–O–O)	441	438	425	430	426	416

In the basis set system (BS-I), the triple–ζ–valence (TZV) basis set[24] is used for the two iron atoms, the TZV plus polarization (TZVP) basis set for the peroxo ligand, and the 3-21G basis set[25–27] for the other H, C, N, and O atoms that are involved in the amino acid residues around the diiron active site. In the basis set system (BS-II), the TZVP basis set for the peroxo ligand is replaced by the TZV basis set in BS-I.

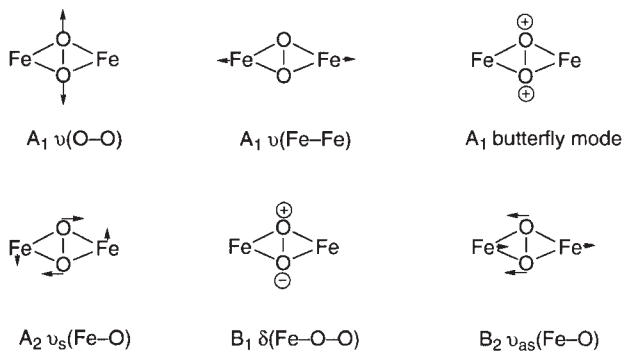

Fig. 4. Vibrational modes of the Fe_2O_2 core in a side-on peroxo complex are estimated from a simple symmetric consideration. ν represents stretches of bonds and δ represents bending.

tions of Fe–O stretching, respectively. The four oxygen-isotope sensitive modes for the side-on peroxo complex **2** are listed in Table 3; symmetric and antisymmetric combinations of the Fe–O stretching, the O–O stretching, and the out-of plane bending modes. Complex **2** shows an O–O stretching mode at 841 cm^{-1} that corresponds to the left-hand side A_1 mode in Fig. 4. The O–O stretching frequency for **2** shifts to 818 and 796 cm^{-1} with $^{16}O^{18}O$ and $^{18}O_2$ substitutions, respectively. A side-on peroxo diiron(III) complex has a high O–O stretching mode relative to those in side-on peroxo dicopper(II) complexes (730–760 cm^{-1}).[32c] The lower O–O stretching frequencies for the side-on peroxo dicopper(II) complexes should be a consequence of some π backbonding of electron density from the two copper atoms into the σ_g* orbital of O_2^{2-}.[32c] Other oxygen-isotope sensitive vibrations are symmetric and antisymmetric combinations of the Fe–O stretching. The frequencies of the symmetric and antisymmetric combinations of the Fe–O stretching were computed to be 506 and 639 cm^{-1}, respectively. The wavenumber 506 cm^{-1} is shifted to 493 cm^{-1} upon $^{18}O_2$ substitution, and the wavenumber 639 cm^{-1} is also shifted to 614 cm^{-1}. The side-on peroxo complex **2** has lower-frequency Fe–O stretching modes relative to those in the end-on peroxo complex **1**. This is because the π-bonding interaction in **2** that makes a significant contribution to the Fe–peroxo bonds is weaker than the σ- and π-bonding interactions in **1**.

We can demonstrate from the DFT calculations that the O–O stretching frequency for the end-on peroxo complex **1** is higher than that for the side-on peroxo complex **2**. If O_2 binds into the active site of MMOH in an end-on *cis*-μ-1,2 fashion, the resonance Raman spectrum of $MMOH_{peroxo}$ should exhibit an oxygen-isotope sensitive vibrational mode at 909 cm^{-1}. On the other hand, an oxygen-isotope sensitive vibrational mode at 841 cm^{-1} is expected to occur if a side-on bridging peroxo ligand is involved at the active site of $MMOH_{peroxo}$. According to DFT calculations, the vibration assigned to the O–O stretching for **1** would shift by 57 cm^{-1} with $^{18}O_2$ labeling, whereas that for **2** would shift by 45 cm^{-1}. Since our DFT calculations suggest that $^{18}O_2$ isotopic shifts strongly depend on the dioxygen bridging modes, $^{18}O_2$ labeling experiments should provide important clues to the geometrical feature of $MMOH_{peroxo}$. The calculated O–O stretching frequency for **1** falls within the range measured in peroxo intermediates of other non-heme diiron enzymes[4–6] and *cis*-μ-1,2 peroxo-bridged diiron(III) synthetic complexes.[8–12] This agreement strongly suggests that the peroxo ligand should coordinate in an end-on *cis*-μ-1,2 fashion rather than a side-on bridging mode in the diiron active site of MMOH. As a consequence, we reasonably predict that O_2

should bind into the active site of $MMOH_{peroxo}$ in an end-on *cis*-μ-1,2 fashion. This prediction is also reasonable from the viewpoint of energetics obtained from DFT calculations, and is consistent with a previous proposal from extended Hückel calculations.[13a–c]

Conclusions

We carried out vibrational analyses for end-on and side-on diiron peroxo complexes as possible models of $MMOH_{peroxo}$ at the B3LYP level of theory. The carboxylate coordination in the active site of MMOH should be responsible for determining the dioxygen bridging mode in $MMOH_{peroxo}$. The end-on peroxo complex with the *cis*-μ-1,2 bridging mode has a doubly bridged structure with two carboxylato ligands, whereas the side-on peroxo complex has one bridging carboxylato ligand. The end-on peroxo complex lies in energy below the side-on peroxo complex. The O–O stretching frequency for the end-on peroxo complex (909 cm^{-1}) is high in comparison with that for the side-on peroxo complex (840 cm^{-1}). The vibrational frequency of the O–O stretching in the end-on peroxo complex shifts by 57 cm^{-1} with $^{18}O_2$ labeling, whereas that in the side-on peroxo complex shifts by 45 cm^{-1}. The present DFT calculations show that the $^{18}O_2$ isotope shifts differ significantly among the dioxygen bridging modes in the active site of MMOH. The O–O stretching frequency in the end-on peroxo complex is in good agreement with those in some *cis*-μ-1,2 peroxo-bridged diiron(III) complexes and the peroxo intermediates in non-heme diiron enzymes. Accordingly, our DFT calculations predict that O_2 should bind in an end-on *cis*-μ-1,2 fashion from the viewpoint of energetics and vibrational frequencies.

K.Y. acknowledges the Ministry of Education, Culture, Sports, Science and Technology, the Japan Society for the Promotion of Science, Japan Science and Technology Cooperation, the Takeda Science Foundation, the Murata Science Foundation, and Kyushu Univeristy P & P "Green Chemistry" for their support of this work. T.Y. thanks the Japan Society for the Promotion of Science for a postdoctral fellowship.

References

1 Reviews on MMO: a) A. L. Feig and S. J. Lippard, *Chem. Rev.*, **94**, 759 (1994). b) J. D. Lipscomb, *Annu. Rev. Microbiol.*, **48**, 371 (1994). c) K. E. Liu and S. J. Lippard, *Adv. Inorg. Chem.*, **42**, 263 (1995). d) B. J. Wallar and J. D. Lipscomb, *Chem. Rev.*, **96**, 2625 (1996). e) L. Que, Jr. and Y. Dong, *Acc. Chem. Res.*, **29**, 190 (1996). f) A. M. Valentine and S. J. Lippard, *J. Chem. Soc., Dalton Trans.*, **1997**, 3925. g) D. M. Kurtz, Jr., *J. Biol. Inorg. Chem.*, **2**, 159 (1997). h) M. Merkx, D. A. Kopp, M. H. Sazinsky, J. L. Blazyk, J. Müller, and S. J. Lippard, *Angew. Chem., Int. Ed.*, **40**, 2782 (2001).

2 a) M. P. Woodland, D. S. Patil, R. Cammack, and H. Dalton, *Biochim. Biophys. Acta*, **873**, 237 (1986). b) A. Ericson, B. Hedman, K. O. Hodgson, J. Green, H. Dalton, J. G. Bentsen, R. H. Beer, and S. J. Lippard, *J. Am. Chem. Soc.*, **110**, 2330 (1988). c) B. G. Fox, K. K. Surerus, E. Münck, and J. D. Lipscomb, *J. Biol. Chem.*, **263**, 10553 (1988). d) A. C. Rosenzweig, C. A. Frederick, S. J. Lippard, and P. Nordlund, *Nature*, **366**, 537 (1993). e) A. C. Rosenzweig, P. Nordlund, P. M. Takahara, C. A. Frederick, and S. J. Lippard, *Chem. Biol.*, **2**, 409 (1995). f) D. A. Whittington and S. J. Lippard, *J. Am. Chem. Soc.*, **123**, 827 (2001).

3 a) K. E. Liu, D. Wang, B. H. Huynh, D. E. Edmondson, A. Salifoglou, and S. J. Lippard, *J. Am. Chem. Soc.*, **116**, 7465 (1994). b) K. E. Liu, A. M. Valentine, D. Qiu, D. E. Edmondson, E. H. Appelman, T. G. Spiro, and S. J. Lippard, *J. Am. Chem. Soc.*, **117**, 4997 (1995). c) K. E. Liu, A. M. Valentine, D. Wang, B. H. Huynh, D. E. Edmondson, A. Salifoglou, and S. J. Lippard, *J. Am. Chem. Soc.*, **117**, 10174 (1995). d) K. E. Liu, A. M. Valentine, D. Qiu, D. E. Edmondson, E. H. Appelman, T. G. Spiro, and S. J. Lippard, *J. Am. Chem. Soc.*, **119**, 11134 (1997). e) S.-K. Lee and J. D. Lipscomb, *Biochemistry*, **38**, 4423 (1999). f) A. M. Valentine, S. S. Stahl, and S. J. Lippard, *J. Am. Chem. Soc.*, **121**, 3876 (1999). g) B. J. Brazeau and J. D. Lipscomb, *Biochemistry*, **39**, 13503 (2000).

4 J. A. Broadwater, J. Ai, T. M. Loehr, J. Sanders-Loehr, and B. G. Fox, *Biochemistry*, **37**, 14664 (1998).

5 P. Moënne-Loccoz, C. Krebs, K. Herlihy, D. E. Edmondson, E. C. Theil, B. H. Huynh, and T. M. Loehr, *Biochemistry*, **38**, 5290 (1999).

6 a) E. I. Solomon, T. C. Brunold, M. I. Davis, J. N. Kemsley, S.-K. Lee, N. Lehnert, F. Neese, A. J. Skulan, Y.-S. Yang, and J. Zhou, *Chem. Rev.*, **100**, 235 (2000). b) E. I. Solomon, *Inorg. Chem.*, **40**, 3656 (2001).

7 J. M. Bollinger, Jr., C. Krebs, A. Vicol, S. Chen, B. A. Ley, D. E. Edmondson, and B. H. Huynh, *J. Am. Chem. Soc.*, **117**, 10174 (1995).

8 T. Ookubo, H. Sugimoto, T. Nagayama, H. Masuda, T. Sato, K. Tanaka, Y. Maeda, H. Okawa, Y. Hayashi, A. Uehara, and M. Suzuki, *J. Am. Chem. Soc.*, **118**, 701 (1996).

9 Y. Dong, S. Yan, V. G. Young, Jr., and L. Que, Jr., *Angew. Chem., Int. Ed. Engl.*, **35**, 618 (1996).

10 K. Kim and S. J. Lippard, *J. Am. Chem. Soc.*, **118**, 4914 (1996).

11 M. Kodera, Y. Taniike, M. Itoh, Y. Tanahashi, H. Shimakoshi, K. Kano, S. Hirota, S. Iijima, M. Ohba, and H. Okawa, *Inorg. Chem.*, **40**, 4821 (2001).

12 a) N. Kitajima, N. Tamura, H. Amagai, H. Fukui, Y. Moro-oka, Y. Mizutani, T. Kitagawa, R. Mathur, K. Heerwegh, C. A. Reed, C. R. Randall, L. Que, Jr., and K. Tatsumi, *J. Am. Chem. Soc.*, **116**, 9071 (1994). b) T. C. Brunold, N. Tamura, N. Kitajima, Y. Moro-oka, and E. I. Solomon, *J. Am. Chem. Soc.*, **120**, 5674 (1998).

13 a) K. Yoshizawa and R. Hoffmann, *Inorg. Chem.*, **35**, 2409 (1996). b) K. Yoshizawa, T. Yamabe, and R. Hoffmann, *New J. Chem.*, **21**, 151 (1997). c) K. Yoshizawa, T. Ohta, T. Yamabe, and R. Hoffmann, *J. Am. Chem. Soc.*, **119**, 12311 (1997). d) K. Yoshizawa, *J. Biol. Inorg. Chem.*, **3**, 318 (1998). e) K. Yoshizawa, T. Ohta, and T. Yamabe, *Bull. Chem. Soc. Jpn.*, **71**, 1899 (1998). f) K. Yoshizawa, A. Suzuki, Y. Shiota, and T. Yamabe, *Bull. Chem. Soc. Jpn.*, **73**, 815 (2000). g) K. Yoshizawa, *J. Inorg. Biochem.*, **78**, 23 (2000). h) K. Yoshizawa and T. Yumura, *Chem.—Eur. J.*, **9**, 2347 (2003).

14 a) P. E. M. Siegbahn and R. H. Crabtree, *J. Am. Chem. Soc.*, **119**, 3103 (1997). b) P. E. M. Siegbahn, R. H. Crabtree, and P. Nordlund, *J. Biol. Inorg. Chem.*, **3**, 314 (1998). c) P. E. M. Siegbahn, *Inorg. Chem.*, **38**, 2880 (1999). d) P. E. M. Siegbahn and M. R. A. Blomberg, *Chem. Rev.*, **100**, 421 (2000). e) P. E. M. Siegbahn, *J. Biol. Inorg. Chem.*, **6**, 27 (2001). f) P. E. M. Siegbahn, *Chem. Phys. Lett.*, **351**, 311 (2002).

15 a) H. Basch, K. Mogi, D. G. Musaev, and K. Morokuma, *J. Am. Chem. Soc.*, **121**, 7249 (1999). b) M. Torrent, D. G. Musaev,

and K. Morokuma, *J. Phys. Chem. B*, **105**, 322 (2001). c) H. Basch, D. G. Musaev, K. Mogi, and K. Morokuma, *J. Phys. Chem. A*, **105**, 3615 (2001). d) M. Torrent, D. G. Musaev, H. Basch, and K. Morokuma, *J. Phys. Chem. B*, **105**, 4453 (2001). e) M. Torrent, K. Mogi, H. Basch, D. G. Musaev, and K. Morokuma, *J. Phys. Chem. B*, **105**, 8616 (2001). f) H. Basch, D. G. Musaev, and K. Morokuma, *J. Phys. Chem. B*, **105**, 8452 (2001). g) M. Torrent, D. G. Musaev, H. Basch, and K. Morokuma, *J. Comput. Chem.*, **23**, 59 (2002). h) M. Torrent, T. Vreven, D. G. Musaev, K. Morokuma, O. Farkas, and H. B. Schlegel, *J. Am. Chem. Soc.*, **124**, 192 (2002).

16 a) B. D. Dunietz, M. D. Beachy, Y. Cao, D. A. Whittington, S. J. Lippard, and R. A. Friesner, *J. Am. Chem. Soc.*, **122**, 2828 (2000). b) B. F. Gherman, B. D. Dunietz, D. A. Whittington, S. J. Lippard, and R. A. Friesner, *J. Am. Chem. Soc.*, **123**, 3836 (2001). c) R. A. Friesner and B. D. Dunietz, *Acc. Chem. Res.*, **34**, 351 (2001). d) V. Guallar, B. F. Gherman, W. H. Miller, S. J. Lippard, and R. A. Friesner, *J. Am. Chem. Soc.*, **124**, 3377 (2002). e) M.-H. Baik, B. F. Gherman, R. A. Friesner, and S. J. Lippard, *J. Am. Chem. Soc.*, **124**, 14608 (2002). f) M.-H. Baik, B. F. Gherman, R. A. Friesner, and S. J. Lippard, *Chem. Rev.*, **103**, 2385 (2003). g) R. A. Friesner, M.-H. Baik, B. F. Gherman, V. Guallar, M. Wirstam, R. B. Murphy, and S. J. Lippard, *Coord. Chem. Rev.*, **238–239**, 267 (2003).

17 a) A. D. Becke, *Phys. Rev. A*, **38**, 3098 (1988). b) A. D. Becke, *J. Chem. Phys.*, **98**, 5648 (1993). c) P. J. Stephens, F. J. Devlin, C. F. Chabalowski, and M. J. Frisch, *J. Phys. Chem.*, **98**, 11623 (1994).

18 C. Lee, W. Yang, and R. G. Parr, *Phys. Rev. B*, **37**, 785 (1988).

19 a) L. Noodleman, *J. Chem. Phys.*, **74**, 5737 (1981). b) L. Noodleman and E. R. Davidson, *Chem. Phys.*, **109**, 131 (1986). c) L. Noodleman, C. Y. Peng, D. A. Case, and J. M. Mouesca, *Coord. Chem. Rev.*, **144**, 199 (1995).

20 M. J. Frisch, G. W. Trucks, H. B. Schlegel, G. E. Scuseria, M. A. Robb, J. R. Cheeseman, V. G. Zakrzewski, J. A. Montgomery, R. E. Stratmann, J. C. Burant, S. Dapprich, J. M. Millam, A. D. Daniels, K. N. Kudin, M. C. Strain, O. Farkas, J. Tomasi, V. Barone, M. Cossi, R. Cammi, B. Mennucci, C. Pomelli, C. Adamo, S. Clifford, J. Ochterski, G. A. Petersson, P. Y. Ayala, Q. Cui, K. Morokuma, D. K. Malick, A. D. Rabuck, K. Raghavachari, J. B. Foresman, J. Cioslowski, J. V. Ortiz, B. B. Stefanov, G. Liu, A. Liashenko, P. Piskorz, I. Komaromi, R. Gomperts, R. L. Martin, D. J. Fox, T. Keith, M. A. Al-Laham, C. Y. Peng, A. Nanayakkara, C. Gonzalez, M. Challacombe, P. M. W. Gill, B. G. Johnson, W. Chen, M. W. Wong, J. L. Andres, M. Head-Gordon, E. S. Replogle, and J. A. Pople, "Gaussian 98," Gaussian Inc., Pittsburgh, PA (1998).

21 a) T. C. Brunold and E. I. Solomon, *J. Am. Chem. Soc.*, **121**, 8277 (1999). b) T. C. Brunold and E. I. Solomon, *J. Am. Chem. Soc.*, **121**, 8288 (1999).

22 a) L. Noodleman and D. A. Case, *Adv. Inorg. Chem.*, **38**, 423 (1992). b) J. M. Mouesca, J. L. Chen, L. Noodleman, D. Bashford, and D. A. Case, *J. Am. Chem. Soc.*, **116**, 11898 (1994). c) J. L. Chen, L. Noodleman, D. A. Case, and D. Bashford, *J. Phys. Chem. A*, **98**, 11059 (1994). d) X. G. Zhao, W. H. Richardson, J. L. Chen, L. Noodleman, H. L. Tsai, and D. N. Hendrickson, *Inorg. Chem.*, **36**, 1198 (1997). e) J. Li, M. R. Nelson, C. Y. Peng, D. Bashford, and L. Noodleman, *J. Phys. Chem. A*, **102**, 6311 (1998). f) T. Lovell, J. Li, and L. Noodleman, *Inorg. Chem.*, **40**, 5251 (2001). g) T. Lovell, J. Li, and L. Noodleman, *Inorg. Chem.*, **40**, 5267 (2001). h) T. Lovell, J. Li, T. Liu, D. A. Case, and L. Noodleman, *J. Am. Chem. Soc.*, **123**, 12392 (2001). i) T. Lovell, W.-G. Han, T. Liu, and L. Noodleman, *J. Am. Chem. Soc.*, **124**, 5890 (2002). j) T. Lovell, J. Li, D. A. Case, and L. Noodleman, *J. Am. Chem. Soc.*, **124**, 4546 (2002).

23 S. H. Vosko, L. Wilk, and M. Nusair, *Can. J. Phys.*, **58**, 1200 (1980).

24 A. Schäfer, C. Huber, and R. Ahlrichs, *J. Chem. Phys.*, **100**, 5829 (1994).

25 J. S. Binkley, J. A. Pople, and W. J. Hehre, *J. Am. Chem. Soc.*, **102**, 939 (1980).

26 M. S. Gordon, J. S. Binkley, J. A. Pople, W. J. Pietro, and W. J. Hehre, *J. Am. Chem. Soc.*, **104**, 2797 (1982).

27 K. D. Dobbs and W. J. Hehre, *J. Comput. Chem.*, **8**, 861 (1987).

28 a) A. P. Scott and L. Radom, *J. Phys. Chem.*, **100**, 16502 (1996). b) M. D. Halls, J. Velkovski, and H. B. Schlegel, *Theor. Chem. Acc.*, **105**, 413 (2001).

29 A computed $\langle S^2 \rangle$ value for the end-on peroxo diiron complex in the broken-symmetry singlet state is 1.00 and 0.19 before and after annihilation of higher spin multiplicites. The J value for this complex was calculated to be 19.5 cm^{-1} by using the following equation, $J = (E_{LS} - E_{HS})/(\langle S^2 \rangle_{HS} - \langle S^2 \rangle_{LS})$; K. Yamaguchi, T. Tsunekawa, Y. Toyoda, and T. Fueno, *Chem. Phys. Lett.*, **143**, 371 (1988).

30 A computed $\langle S^2 \rangle$ value for the side-on peroxo diiron complex in the broken-symmetry singlet state is 1.07 and 0.55 before and after annihilation of higher spin multiplicites. The J value for this complex was calculated to be 248.8 cm^{-1}, which is larger than that for the end-on peroxo complex.

31 a) M. J. Baldwin, D. E. Root, J. E. Pate, K. Fujisawa, N. Kitajima, and E. I. Solomon, *J. Am. Chem. Soc.*, **114**, 10421 (1992). b) E. I. Solomon, F. Tuczek, D. E. Root, and C. A. Brown, *Chem. Rev.*, **94**, 827 (1994). c) E. I. Solomon, P. Chen, M. Metz, S.-K. Lee, and A. E. Palmer, *Angew. Chem., Int. Ed.*, **40**, 4570 (2001).

32 K. A. Magnus, B. Hazes, H. Ton-That, C. Bonaventura, J. Bonaventura, and W. G. J. Hol, *Proteins*, **19**, 302 (1994).

33 J. Ling, L. P. Nestor, R. S. Czernuszewicz, T. G. Spiro, R. Fraczkiewicz, K. D. Sharma, T. M. Loehr, and J. Sanders-Loehr, *J. Am. Chem. Soc.*, **116**, 7682 (1994).

34 N. Kitajima, K. Fujisawa, C. Fujimoto, Y. Moro-oka, S. Hashimoto, T. Kitagawa, K. Toriumi, K. Tatsumi, and A. Nakamura, *J. Am. Chem. Soc.*, **114**, 1277 (1992).

35 S. Mahapatra, J. A. Halfen, E. C. Wilkinson, L. Que, Jr., and W. B. Tolman, *J. Am. Chem. Soc.*, **116**, 9785 (1994).

36 E. Pidcock, H. V. Obias, C. X. Zhang, K. D. Karlin, and E. I. Solomon, *J. Am. Chem. Soc.*, **120**, 7841 (1998).

37 P. K. Ross and E. I. Solomon, *J. Am. Chem. Soc.*, **113**, 3246 (1991).

38 F. A. Cotton, "Chemical Applications of Group Theory," Wiley-Interscience, New York (1997).

39 F. Neese and E. I. Solomon, *J. Am. Chem. Soc.*, **120**, 12829 (1998).